Geochemical Perspectives Letters

Graphite floatation on a magma ocean and the fate of carbon during core formation

H. Keppler[1*], G. Golabek[1]

OPEN ACCESS
doi: 10.7185/geochemlet.1918

Abstract

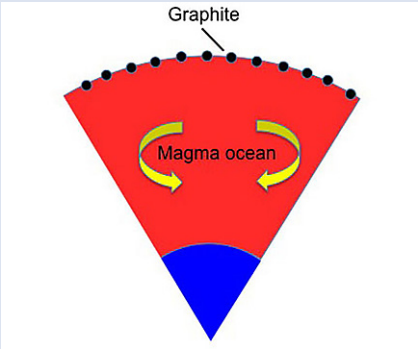

Carbon is a strongly siderophile element and current models assume that in a magma ocean, most of the carbon is sequestered into the core. Here we show that (i) for an initially highly reduced magma ocean, most of the carbon will be reduced to graphite, which is less dense than a peridotite melt; (ii) the graphite can be dynamically stable at the surface of a magma ocean; (iii) the equilibrium of the primordial atmosphere with graphite buffers CO and CO_2 fugacity to such low values, that only traces of carbon dissolve in the magma ocean. Therefore, under very reducing conditions, most of the carbon may remain near the surface during core formation of a terrestrial planet and the extent of carbon sequestration into the core may be limited. We suggest that the ureilite meteorites may be the remnants of such a graphite-rich surface layer on a partially or completely molten planetesimal. A similar, graphite-enriched surface may also exist on Mercury.

Received 21 March 2019 | Accepted 7 June 2019 | Published 9 July 2019

Introduction

The initial distribution of carbon in terrestrial planets was likely affected by processes occurring during the formation and solidification of a magma ocean (Elkins-Tanton, 2012). Carbon is known to be siderophile and a number of studies have therefore investigated the partitioning of carbon between a silicate melt and iron metal (Dasgupta and Walker 2008; Dasgupta *et al.*, 2013; Chi *et al.*, 2014). Measured partition coefficients $D_C^{metal/silicate}$ typically range from 500 to 5000. Accordingly, current models assume that during the evolution and solidification of the magma ocean, most of the carbon is sequestered into the core, leaving a carbon-depleted silicate mantle and primordial atmosphere behind (Dasgupta, 2013; Hirschmann, 2016).

The redox state of a magma ocean depends largely on the type of material accreted. Heterogeneous accretion models are required to meet constraints imposed by trace element concentrations in the present day mantle and experimentally determined trace element partition coefficients. The models of Rubie *et al.* (2011, 2015) suggest that Earth´s formation started with the accretion of highly reduced material, while more oxidised material was added later. This corresponds to an initial oxygen fugacity 5.5 log units below the iron-wustite buffer (IW-5.5), while during the late stages of accretion, oxygen fugacity increased to IW-2. During the later stages of accretion, most mass was delivered by large impactors and full equilibrium between metal and silicate melt was not achieved. Therefore, the partitioning of carbon into the core mostly occurred early in a very reducing environment. Carbon in chondritic meteorites is mostly present in the form of some carbonaceous, graphite-like material. Figure 1 illustrates the consequences of chemical equilibrium between a reduced magma ocean and graphite when a gas phase is present. The equilibrium between a CO-CO_2 gas phase and graphite is given by the CCO buffer. The oxygen fugacity imposed by this buffer depends strongly on the CO + CO_2 gas pressure. In equilibrium, the oxygen fugacity of the magma ocean, which is controlled by the concentration and redox state of iron, has to be the same as the oxygen fugacity of the CCO buffer. Figure 1 shows that for example at 2000 K, a magma ocean with an oxygen fugacity 4 log units below the Fe-FeO (iron-wustite, IW) buffer would limit the CO + CO_2 pressure coexisting with graphite to 100 bars; at 1600 K, the corresponding value would be just 10 bars. The carbon content in carbonaceous chondrites ranges from 0.1 to >5 wt. %, with an average near 2.9 wt. % (Kerridge, 1985). If the bulk Earth included just 2 % of such volatile-rich material (Marty, 2012) and if all this carbon were converted into a CO-CO_2 gas phase, the resulting gas pressure would be in the range of 1600 to 2500 bar, depending on the CO_2/CO ratio. Obviously, if oxygen fugacity is controlled by a reduced magma ocean, the resulting low CO + CO_2 pressures imply that most of the carbon must be reduced to graphite.

1. Bayerisches Geoinstitut, Universität Bayreuth, 95440 Bayreuth, Germany
* Corresponding author (email: hans.keppler@uni-bayreuth.de)

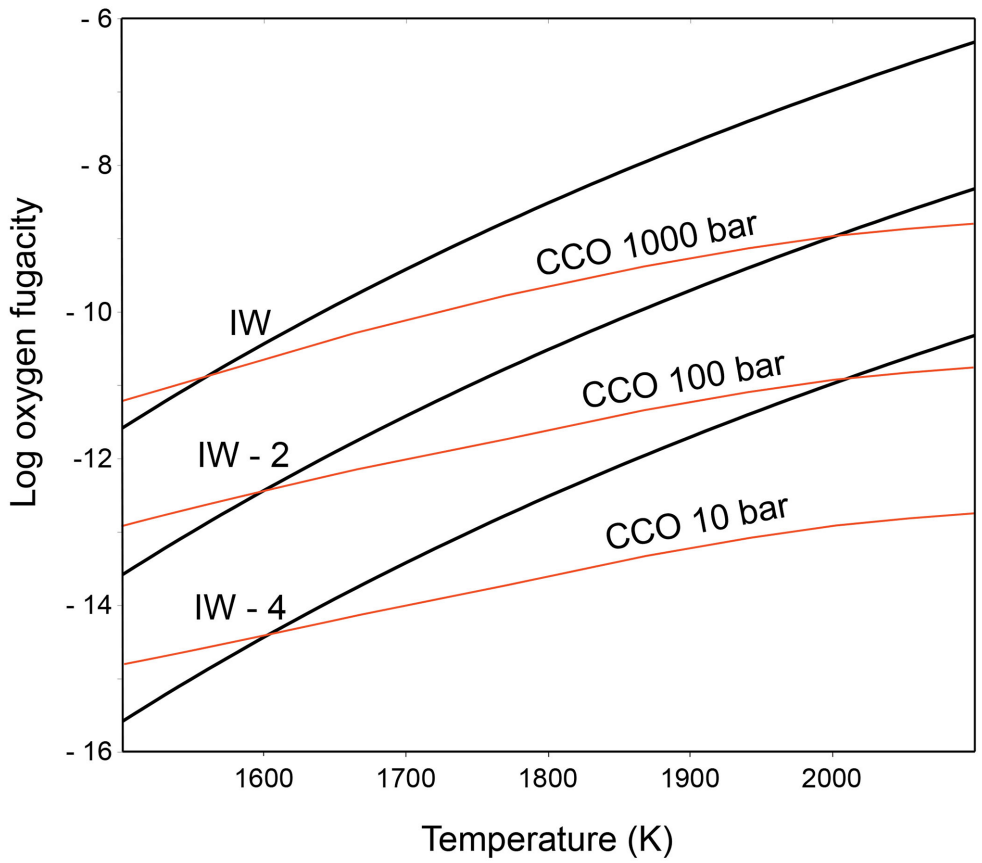

Figure 1 Consequences of thermodynamic equilibrium between a magma ocean, graphite, and a primordial atmosphere. Shown are the curves for the oxygen fugacities of the iron-wustite (Fe-FeO) buffer (IW) and for the graphite–CO–CO_2 buffer (CCO) for different CO + CO_2 pressures (see Methods in Supplementary Information). Plausible oxygen fugacities of a magma ocean range from IW-2 to IW-5.5 (Rubie *et al.*, 2011). The diagram shows that equilibrium between such a reducing magma ocean and graphite buffers the CO + CO_2 pressure in a primordial atmosphere to very low values.

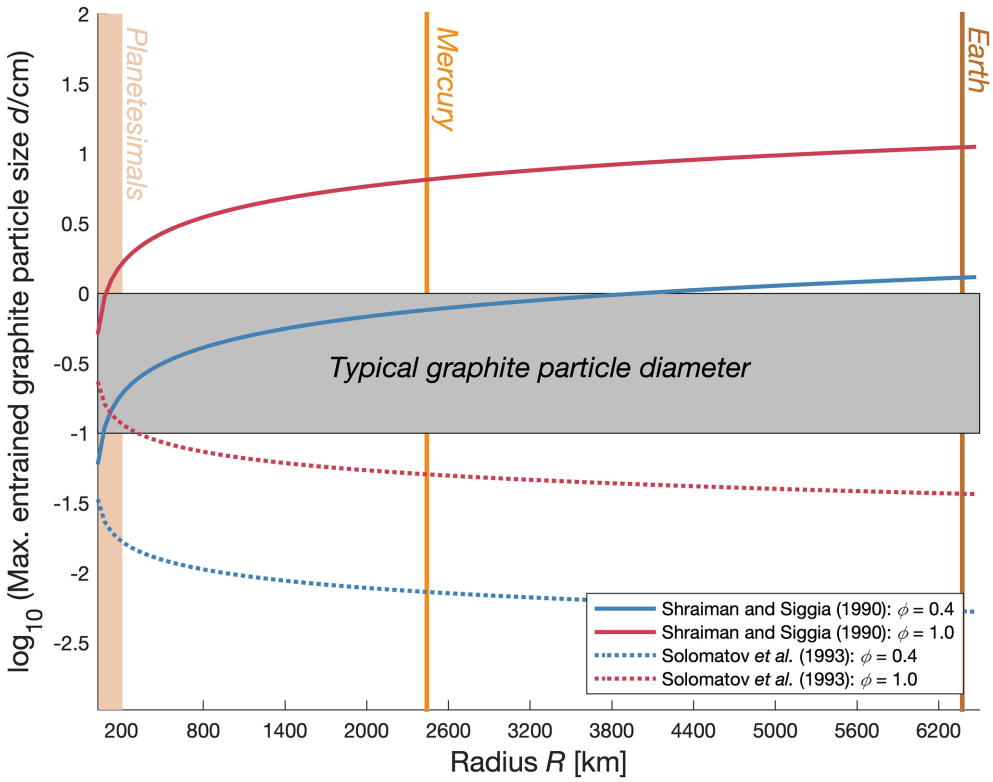

Figure 2 Two estimates for the diameter of the largest graphite particles that can be entrained in both a partially (φ = 0.4) and a fully molten (φ = 1.0) convecting magma ocean for planetary objects ranging from 25 km radius up to Earth's radius. The grey band indicates typical diameters of graphite particles found in meteorites.

Dynamic Stability of Graphite at the Surface of a Magma Ocean

The density of graphite (2250 kg/m^3 at ambient conditions) is significantly smaller than that of peridotite melt (2700 kg/m^3 at 2000 K; Courtial *et al.*, 1997). Therefore, it appears plausible that graphite would float on the surface of a magma ocean. Indeed, the density difference between graphite and peridotite melt is much higher than that for plagioclase (with a density of 2600 - 2700 kg/m^3 at ambient conditions). Plagioclase floatation on a lunar magma ocean is widely believed to be responsible for the formation of the anorthosite crust of the Moon (*e.g.*, Elkins-Tanton *et al.*, 2011). Accordingly, it would be rather surprising if graphite did not accumulate at the surface of a magma ocean.

We have studied the potential rise of graphite particles in a magma ocean following the two approaches described by Solomatov *et al.* (1993) and by Shraiman and Siggia (1990); see Methods in Supplementary Information for details. For planetary objects ranging from a radius of 25 km up to that of the Earth, we estimated the maximum diameter of particles that can be entrained in the magma ocean and compare the results with the typical diameter of graphite grains or aggregates in meteorite samples (see Fig. 2). The results indicate that graphite particle floatation is viable when considering the equation given by Solomatov *et al.* (1993), while using the equation of Shraiman and Siggia (1990) graphite floatation would be only possible in small planetary objects. However, allowing for some sintering of graphite into larger aggregates at the surface of a magma ocean, graphite floatation will be possible in all cases.

The Fate of Carbon in a Magma Ocean Covered by Floating Graphite

Figure 3a shows the fugacities of CO and CO_2 in equilibrium with graphite at various oxygen fugacities and the resulting carbon solubility in the silicate melt (see Methods, Supplementary Information). Under very reducing conditions, predicted carbon solubilities are very low. At 2000 K and IW-6, only 0.15 ppm C is in the melt. The solubility rises to about 1 ppm near IW-4 and to 19 ppm at IW-2. However, the partition coefficient of carbon between the metal phase and the silicate melt also depends on oxygen fugacity. Figure 3b shows the predicted $D^{metal/silicate}$ according to the numerical regression model by Chi *et al.* (2014). For a peridotite melt with a structural parameter (non-bridging oxygen atoms per tetrahedron) of $NBO/T = 3$, 2000 K and 3 GPa, the partition coefficient increases from about 1100 at IW-2 to 2.6 x 10^5 at IW-6. This means that the metal in equilibrium with the silicate melt should contain 2 – 4 wt. % carbon, nearly independent of oxygen fugacity (Fig. 3b). This shows that the thermodynamic models involved in the calculation are reliable. Since the metal phase is in equilibrium with the silicate melt, which in turn is in equilibrium with graphite, the carbon content in the molten metal should be the same as if the metal were in direct equilibrium with graphite. Indeed, the stable phase diagram of the Fe-C system at ambient pressure shows that liquid iron in equilibrium with graphite contains between 5 and 6 wt. % C at 2000 K (Okamoto *et al.*, 1992). This is in satisfactory agreement with the predicted carbon content as shown in Figure 3b, considering that this calculation involves a rather large extrapolation of the partitioning model of Chi *et al.* (2014) to more reducing conditions.

The concentrations of carbon in metal as predicted in in Figure 3b would imply that irrespective of redox conditions, most of the carbon in a growing planet would be sequestered into the core, if full thermodynamic equilibrium between the metal melt, the magma ocean and the atmosphere is reached, in agreement with previous models (Dasgupta, 2013; Hirschmann, 2016). Since the carbon concentration in the silicate melt in equilibrium with graphite is very low, however, this would require continuous replenishment of carbon in the melt during the entire time required to reach equilibrium with the metal. This is extremely unlikely to occur, since metal droplets in a magma ocean rapidly sink towards the core, while re-equilibration of the melt with the graphite and the atmosphere on the surface is only possible with a full convective overturn. Only if metal remained suspended in the melt during several convective overturns, could the predicted equilibrium concentration of carbon in the metal phase be reached. Due to the large density difference between metal and silicate melt, this is unlikely to occur, except perhaps for a small fraction or for very small droplets (see also Fig. 3 in Lichtenberg *et al.*, 2018).

A more plausible scenario for the sequestration of carbon into the core is therefore that the metal phase during its descent towards the core only extracts the carbon that is already present in the silicate melt. In such a case, the possible concentrations of carbon in the metal are limited by mass balance. If for example, the mass ratio between newly added impactor metal and the mass of the magma ocean is 1:1000, and the melt contains 1 ppm of carbon (at IW-4), then the maximum possible concentration of carbon in the metal is 1000 ppm, if all carbon completely partitioned into the metal. It should be noted that in this model, the possible concentration of carbon in the core is limited by incomplete equilibration with the graphite and the atmosphere on the surface; this is a completely different effect to the limited equilibration between metal and silicate melt (due to limited diffusion paths in either phase), which has been invoked in previous models (*e.g.*, Rubie *et al.*, 2011).

The maximum carbon concentration that may be reached in the core of a growing planet, if the accreted metal only extracts the carbon present in the silicate melt phase of the magma ocean, can be easily calculated. We assume that the accretion of a planet with final mass M involves N equal-mass impact events. The metal added rapidly sinks to the core; after reaching the core, there is no further equilibration, as assumed in all current models of core formation (*e.g.*, Rubie *et al.*, 2011, 2015). The average carbon concentration in the core after complete accretion is then

$$\overline{C_m} = c_s(N + 1)\,\frac{1 - f}{f}$$

where f is the fraction of metal in the impactor, which we assume to be constant and c_s is the equilibrium concentration of carbon in the silicate melt (see Methods in the Supplementary Information for the derivation of this equation).

Figure 4 shows the predicted maximum carbon concentrations in the core for different oxygen fugacities as a function of the total number of impact events N. Accretion simulations (Rubie *et al.*, 2015) suggest that for terrestrial planets, the number of impacts by planetary embryos ranges between 70 and 210, which is within the range covered by Figure 4. The metal fraction in the accreting material was assumed to be $f = 0.32$, as in the Earth. Figure 4 also shows the fraction of total carbon in a planet ending up in the core, assuming a bulk carbon content of 500 ppm by weight, as inferred for the Earth (Marty, 2012).

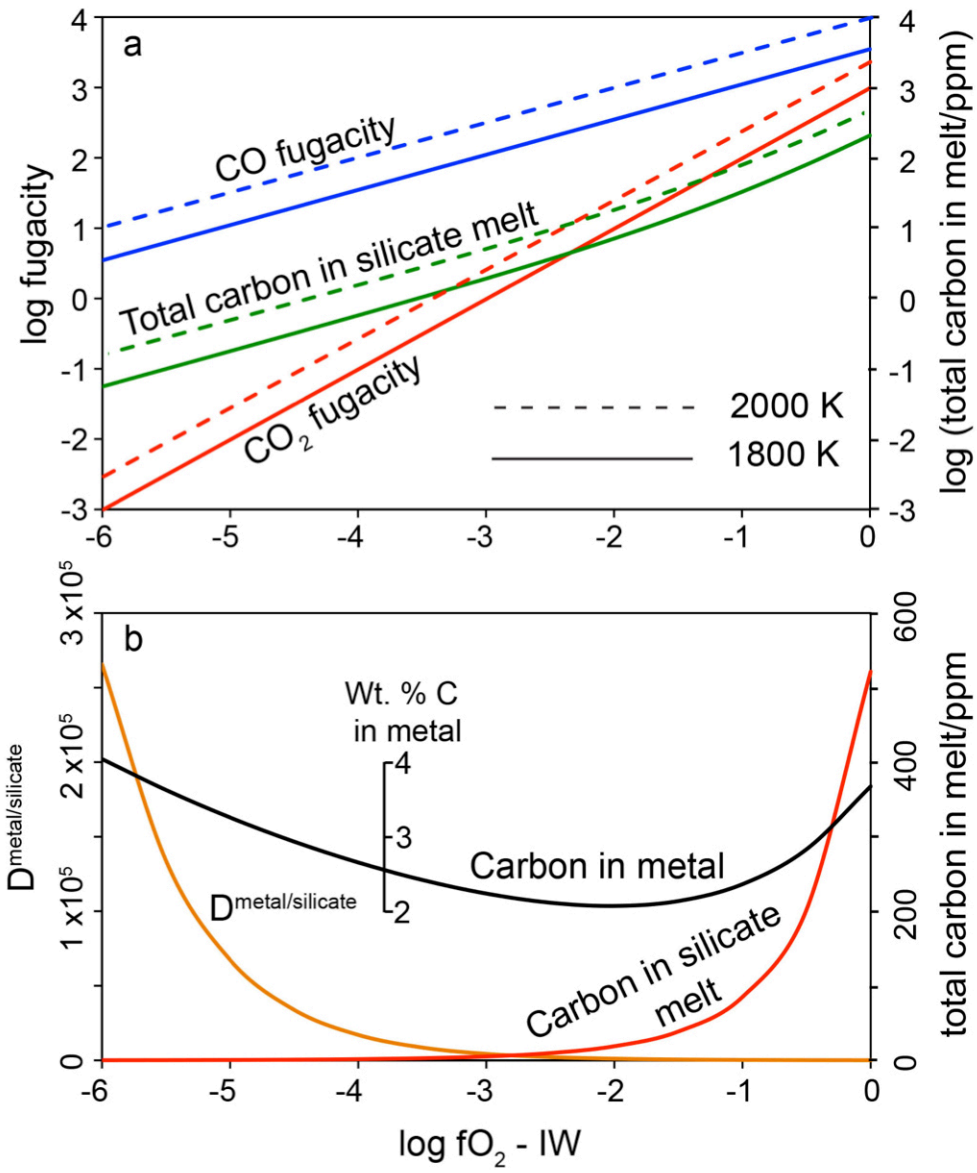

Figure 3 Partitioning of carbon between atmosphere, silicate melt, and metal in the presence of graphite. **(a)** CO fugacity, CO_2 fugacity, and total carbon in a silicate melt in equilibrium with graphite for a temperature of 1800 and 2000 K at the surface of a magma ocean. **(b)** Carbon content in the silicate melt as expected from the equilibrium with graphite at 2000 K at the surface of a magma ocean, predicted metal/silicate melt partition coefficient of carbon inside the magma ocean (after Chi *et al.*, 2014, NBO/T = 3, 2000 K and 3 GPa) and predicted carbon content of metal in equilibrium with the silicate melt. In the presence of hydrogen, methane could be an additional carbon species; however, as we show in the Supplementary Information, the effect of CH_4 on the behaviour of carbon is likely negligible.

Carbon in the Early Earth, on Mercury, and a Possible Origin for Ureilites

Figure 4 illustrates that the fate of carbon in a terrestrial planet strongly depends on the redox state prevailing during accretion and on the number of impacts of planetary embryos. Every impact sequestrates carbon from the graphite saturated magma ocean, thus the larger the number of individual impacts, the more efficiently is carbon transferred into the core. However, Figure 4 shows that even a very large number of impacts will only transfer ≈25 % or less of the total carbon of a terrestrial planet into the core, if the oxidation state of the magma ocean is below IW-4. For IW-3, between about 25 and 75 % of the total carbon may be sequestered into the core for a range of impact events between about 70 and 210 (Rubie *et al.*, 2015). Only at a higher oxidation state of IW-2, could sequestration of carbon into the core be nearly complete. However, it is important to note that the curves given in Figure 4 are effectively upper limits of carbon concentrations in the core, as they assume that (i) the impacting metal extracts all carbon from the entire magma ocean and (ii) the metal fully equilibrates with the silicate melt. However, Deguen *et al.* (2011, 2014) show that for smaller impacts, the metal equilibrates only with part of the magma ocean and for large impacts only a fraction of the metal equilibrates. Both effects will limit the sequestration of carbon into the core, such that even at IW-2, some carbon will likely remain near the planetary surface.

For the Earth, accretion likely started at IW-5.5 with a gradual increase of oxidation state up to IW-2 during the final stage (Rubie *et al.*, 2011). However, towards the end of accretion, above IW-3, equilibration of large impactor cores with the magma ocean became inefficient. Figure 4 therefore suggests that a significant fraction of total carbon, possibly as much as 50 % did not enter the core. Since carbon solubility in the silicate melt is very low, this carbon would likely have remained as a graphite layer in equilibrium with a primordial atmosphere

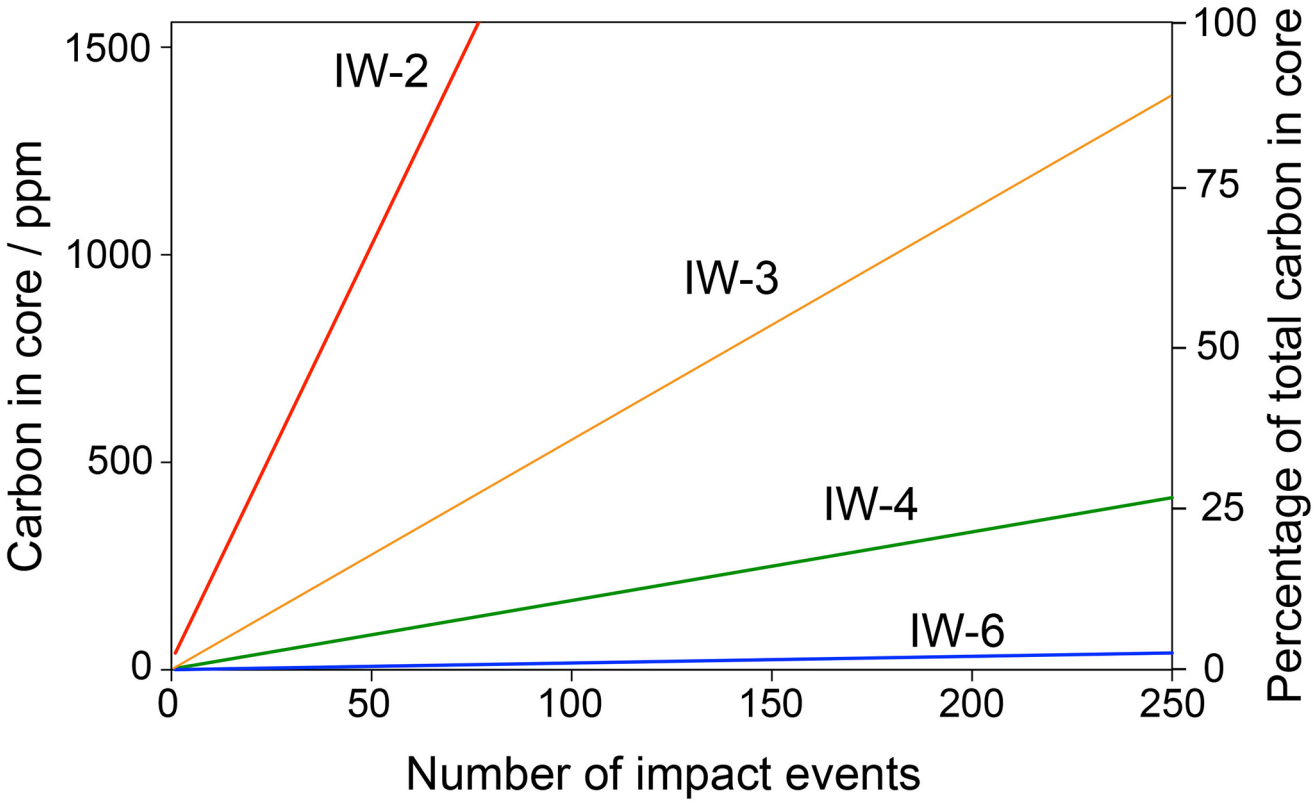

Figure 4 The fate of carbon during core formation of a terrestrial planet. Maximum possible carbon content in the core as a function of the number of impact events by planetary embryos, for oxygen fugacities from IW-6 to IW-2 and a surface temperature of 2000 K (left scale); predicted maximum fraction of total carbon sequestered in the core (right scale) for a terrestrial planet with a bulk carbon content of 500 ppm (Marty, 2012).

near the planetary surface. We suggest that the ureilites, a group of ultramafic, achondritic meteorites (Goodrich, 1992) that typically contain several percent of graphite and experienced at least some partial melting (*e.g.*, Singletary and Grove, 2003; Wilson *et al.*, 2008) may be the remnants of such a graphite-rich layer at the surface of a planet that went through a magma ocean stage involving graphite floatation on the surface. The carbon-rich nature of these meteorites may well be explained by the floatation of graphite at the surface of a magma ocean, where the graphite then got incorporated into an incompletely molten crust. Remote sensing data suggest that a similar carbon-enriched crust may exist on the surface of Mercury (Peplowski *et al.*, 2016; see also Fig. 2 and the Supplementary Information).

Conclusions

We show that the equilibrium between a highly reducing magma ocean and a primordial, carbon-rich atmosphere necessarily leads to the precipitation of graphite, floating on top of the magma ocean. The graphite buffers the solubility of carbon in the silicate melt to such low values that the sequestration of carbon into the core becomes inefficient. A terrestrial planet may therefore solidify with a graphite-rich layer at the surface that retains most of the carbon inventory. This layer may reduce planetary albedo and therefore enhance surface temperatures. Moreover, the concentration of graphite near the surface may be a viable mechanism for the selective loss of carbon by impact erosion. The ureilite meteorites may be samples of the graphite-enriched surface of an asteroid that experienced a magma ocean stage.

Acknowledgements

Constructive reviews by Bruno Scaillet and an anonymous referee helped to improve this manuscript.

Editor: Ambre Luguet

Additional Information

Supplementary Information accompanies this letter at http://www.geochemicalperspectivesletters.org/article1918.

Cite this letter as: Keppler, H., Golabek, G. (2019) Graphite floatation on a magma ocean and the fate of carbon during core formation. *Geochem. Persp. Let.* 11, 12–17.

References

Chi, H., Dasgupta, R., Duncan, M.S., Shimizu, N. (2014) Partitioning of carbon between Fe-rich alloy melt and silicate melt in a magma ocean - Implications for the abundance and origin of volatiles in Earth, Mars, and the Moon. *Geochimica et Cosmochimica Acta* 139, 447–471.

Courtial, P., Ohtani, E. Dingwell, D.B. (1997) High-temperature densities of some mantle melts. *Geochimica et Cosmochimica Acta* 61, 3111–3119.

Dasgupta, R. (2013) Ingassing, storage, and outgassing of terrestrial carbon through geologic time. *Reviews in Mineralogy and Geochemistry* 75, 183–229.

Dasgupta, R., Walker, D. (2008) Carbon solubility in core melts in a shallow magma ocean environment and distribution of carbon between the Earth's core and the mantle. *Geochimica et Cosmochimica Acta* 72, 4627–4641.

Dasgupta, R., Chi, H., Shimizu, N., Buono, A.S., Walker, D. (2013) Carbon solution and partitioning between metallic and silicate melts in a shallow magma ocean: Implications for the origin and distribution of terrestrial carbon. *Geochimica et Cosmochimica Acta* 102, 191–212.

Deguen, R., Olson, P., Cardin, P. (2011) Experiments on turbulent metal-silicate mixing in a magma ocean. *Earth and Planetary Science Letters* 310, 303–313.

Deguen, R., Landeau, M., Olson, P. (2014) Turbulent metal-silicate mixing, fragmentation, and equilibration in magma oceans. *Earth and Planetary Science Letters* 391, 274–228.

Elkins-Tanton, L.T. (2012) Magma oceans in the inner solar system. *Annual Review of Earth and Planetary Sciences* 40, 113–139.

Elkins-Tanton, L.T., Burgess, S., Yin, Q.Z. (2011) The lunar magma ocean: Reconciling the solidification process with lunar petrology and geochronology. *Earth and Planetary Science Letters* 304, 326–336.

Goodrich, C.A. (1992) Ureilites - a critical-review. *Meteoritics* 27, 327–352.

Hirschmann, M.M. (2016) Constraints on the early delivery and fractionation of Earth's major volatiles from C/H, C/N, and C/S ratios. *American Mineralogist* 101, 540–553.

Kerridge, J.F. (1985) Carbon, hydrogen and nitrogen in carbonaceous chondrites: Abundances and isotopic compositions in bulk samples. *Geochimica et Cosmochimica Acta* 49, 1707–1714.

Lichtenberg, T. Golabek, G.J., Dullemond, C.P., Schönbächler, M., Gerya, T.V., Meyer, M.R. (2018) Impact splash chondrule formation during planetesimal recycling. *Icarus* 302, 27–43.

Marty, B. (2012) The origins and concentrations of water, carbon, nitrogen and noble gases on Earth. *Earth and Planetary Science Letters* 313–314, 56-66.

Okamoto, H. (1992) The C-Fe (carbon-iron) system. *Journal of Phase Equilibria* 13, 543–565.

Peplowski, P.N., Klima, R.L., Lawrence, D.J., Ernst, C.M., Denevi, B.W., Frank, E.A., Goldsten, J.O., Murchie, S.L., Nittler, L.R., Solomon, S.C. (2016) Remote sensing evidence for an ancient carbon-bearing crust on Mercury. *Nature Geoscience* 9, 273–276.

Rubie, D.C., Frost, D.J., Mann, U., Asahara, Y., Nimmo, F., Tsuno, K., Kegler, P., Holzheid, A., Palme, H. (2011) Heterogeneous accretion, composition and core–mantle differentiation of the Earth. *Earth and Planetary Science Letters* 301, 31–42.

Rubie, D.C., Jacobson, S.A., Morbidelli, A., O'Brien, D.P., Young, E.D., Devries, J., Nimmo, F., Palme, H., Frost, D.J. (2015) Accretion and differentiation of the terrestrial planets with implications for the compositions of early-formed Solar System bodies and accretion of water. *Icarus* 248, 89–108.

Shraiman, B.I., Siggia, E.D. (1990) Heat transport in high-Rayleigh-number convection. *Physical Review A* 42, 3650–3653.

Singletary, S.J., Grove, T.L. (2003) Early petrologic processes on the ureilite parent body. *Meteoritics and Planetary Science*, 38, 95–108.

Solomatov, V.S., Olson, P., Stevenson, D.J. (1993) Entrainment from a bed of particles by thermal convection. *Earth and Planetary Science Letters* 120, 387–393.

Wilson, L., Goodrich, C.A., Van Orman, J.A. (2008) Thermal evolution and physics of melt extraction on the ureilite parent body. *Geochimica et Cosmochimica Acta* 72, 6154–6176.

Geochemical Perspectives Letters

Graphite floatation on a magma ocean and the fate of carbon during core formation

H. Keppler, G. Golabek

Supplementary Information

The Supplementary Information includes:

- Methods
- Supplementary discussion
- Figure S-1
- Supplementary Information References

Methods

Calculation of the dynamic stability of graphite particles at the surface of a magma ocean

We studied the potential rise of graphite particles in a magma ocean following the method described in detail in Solomatov (2015). The convective heat flux q of the magma ocean can be calculated as

$$q = 0.089k\frac{(T_m - T_0)Ra^{1/3}}{D} \quad \text{(Eq. S-1)}$$

with the Rayleigh number

$$Ra = \left[\frac{\alpha_{Si} g \rho_{Si}(T_m - T_0)D^3}{\kappa\eta}\right] \quad \text{(Eq. S-2)}$$

and the thermal expansivity of the silicate melt α_{Si}, gravity acceleration $g = 4/3\pi\rho GR$, with silicate melt density $\rho_{Si} \approx 2700$ kg/m^3, G being Newton's constant, R the radius of the planetary object, potential temperature T_m, assumed surface temperature of space T_0 = 290 K, thermal diffusivity $\kappa = k/(\rho_{Si}c_P)$, thermal conductivity of silicates k, silicate melt heat capacity c_P and depth of the magma D. For the calculation of the gravity acceleration g close to the surface of each planetary object we use an average density $\rho = \rho_{Si} + (\rho_{Fe} - \rho_{Si})(D/R)^3$ assuming that each object is differentiated into an iron core with radius $R/2$ and density ρ_{Fe} and a magma ocean on top with silicate melt density ρ_{Si} and thickness $D = R/2$. At the rheological transition (melt fraction $\phi > 0.4$-0.6) the viscosity η in a magma ocean drops by orders of magnitude from $\eta \approx 10^{17}$ Pa s to $\approx 10^{-2}$ Pa s (Rubie *et al.*, 2003; Liebske *et al.*, 2005). The convective velocity in the magma ocean (Priestly, 1959; Kraichnan, 1962) is given as

$$v_S \approx 0.6\left(\frac{\alpha_{Si} g l q}{\rho_{Si} c_P}\right)^{1/3} \quad \text{(Eq. S-3)}$$

with mixing length $l \approx D \approx R/2$.

We used the results of two laboratory experiments to estimate the size of graphite particles that can be suspended by convective flow. Based on Shraiman and Siggia (1990) the largest entrained graphite particles have a diameter given as

$$d \leq \frac{\rho_{Si}\left(\frac{v_S}{x^*}\right)^2}{0.1\left(\rho_{Si} - \rho_G\right) g} \quad \text{(Eq. S-4)}$$

with graphite density $\rho_G \approx 2250$ kg/m^3 and constant factor $x^* = 60$. Using the results by Solomatov *et al.* (1993) we obtain the following equation for the diameter of the largest entrained graphite particles

$$d \leq \frac{\left(\frac{\eta_l \alpha_{Si} q}{c_P}\right)^{1/2}}{0.1\left(\rho_{Si} - \rho_G\right) g^{1/2}} \quad \text{(Eq. S-5)}$$

where η_l is the viscosity of silicate melt set to 10^{-2} Pa s (Rubie *et al.*, 2003; Liebske *et al.*, 2005).

Thermodynamic calculation of carbon solubility in a magma ocean in equilibrium with graphite

The fugacities of CO and CO_2 in equilibrium with graphite are controlled by the two equilibria

$$C + \tfrac{1}{2} O_2 = CO \quad \text{(Eq. S-6)}$$

$$C + O_2 = CO_2 \quad \text{(Eq. S-7)}$$

Obviously, if the oxygen fugacity is imposed by the oxidation state of the magma ocean, the fugacities of both CO and CO_2 are fixed at a given temperature and can be readily calculated using the thermodynamic data for CO and CO_2 tabulated in Robie and Hemingway (1995). The oxygen fugacity of the IW (Fe-FeO buffer; Fig. 1) was calculated from the thermodynamic data of FeO in Robie and Hemingway (1995).

The solubilities of CO and CO_2 in a silicate melt follow Henry´s law, i.e. the dissolved concentrations c of CO and CO_2 are directly proportional to their fugacity in the gas phase. Therefore

$$c_C^{melt} = K_{CO} f_{CO} + K_{CO2} f_{CO2} \quad \text{(Eq. S-8)}$$

where K_{CO} and K_{CO2} are the Henry constants of CO and CO_2, respectively, expressed as ppm carbon per bar, and f_{CO} and f_{CO2} are the fugacities of CO and CO_2. The solubility of CO_2 in silicate melts may be described by $K_{CO2} = 0.155$ ppm C/bar for a wide range of compositions (Ni and Keppler 2013). Yoshioka *et al.* (2019) found that the CO solubility in MORB melt may be described by the equation $\log c_{CO} = -5.20 + 0.80 \log f_{CO}$ ($R^2 = 0.83$) with c_{CO} being expressed as carbon in wt. %. Since the coefficient in front of the log f_{CO} term is close to 1, at low pressures this relationship may also be approximately described by a Henry constant of $K_{CO} = 0.016$ ppm C/bar. While this Henry constant is based on experiments with MORB melt, the study of Yoshioka *et al.* (2019) suggests that the solubility is not very dependent on melt composition and therefore, the same solubility law may be used as a reasonable approximation for a peridotite melt. With these assumptions, the carbon solubilities in Figure 2 were calculated from equation S-8.

Calculation of carbon extraction from the magma ocean during core formation

The maximum carbon concentration that may be reached in the core of a growing planet, if the accreted metal only extracts the carbon present in the silicate melt phase of the magma ocean can be easily calculated. We assume that the accretion of a planet with final mass M occurs in N equal steps; i.e. there are N impact events, which cause the planet to grow. This means that the mass m_m of metal added during each step is

$$m_m = \frac{Mf}{N} \quad \text{(Eq. S-9)}$$

where f is the fraction of metal in the impactor, which we assume to be constant. The metal added rapidly sinks to the core; after reaching the core, there is no further equilibration, as assumed in all current models of core formation (e.g. Rubie *et al.* 2011, 2015).

The mass of the silicate melt m_s in a deep magma ocean extending down to the mantle core boundary after the nth impact event is then

$$m_s = \frac{nM(1-f)}{N} \quad \text{(Eq. S-10)}$$

The equilibrium concentration of carbon in the silicate melt, as adjusted by the equilibrium with graphite and the gas phase on the surface is c_s; due to the very high metal/silicate partition coefficients of carbon under reducing conditions (see Fig. 3b), one may assume in good approximation that almost all of the carbon originally present in the melt is sequestered by the metal phase, yielding the carbon concentration in the metal c_m for the nth impact

$$c_m = c_s \frac{m_s}{m_m} = c_s n \frac{1-f}{f} \quad \text{(Eq. S-11)}$$

The average carbon concentration in the core after complete accretion is then

$$\overline{c_m} = \frac{1}{N}\sum_{n=1}^{N} c_s n \frac{1-f}{f} = c_s (N+1)\frac{1-f}{2f} \quad \text{(Eq. S-12)}$$

Discussion

Carbon solubility in a magma ocean in the presence of methane

The model calculations for the behavior of carbon in a magma ocean as outlined in this study are based on the simple C-O system, where the fugacities are controlled by the equilibrium of the gas phase with graphite and the magma ocean. These fugacities will not change if other volatile components are present. However, in the presence of water or hydrogen, some methane may form as additional species, which may contribute to bulk carbon solubility. According to the equilibrium

$$C + 2\,H_2 = CH_4 \quad \text{(Eq. S-13)}$$

the fugacity of methane in equilibrium with graphite is controlled by the fugacity of hydrogen (H_2). In Figure S-1a, we calculated methane fugacity for a range of temperatures and H_2 fugacities from 1 to 1000 bar, using the thermodynamic data from Robie and Hemingway (1995). The diagram shows that in order to stabilize appreciable amounts of CH_4, very high hydrogen fugacities are required. This is due to the fact that the Gibbs free energy of formation of methane at high temperature is distinctly positive.

The solubility of methane in a basaltic melt at 1400 °C was studied by Ardia *et al.* (2013). At low pressures, their data suggest a Henry constant for methane of 138.4 ppm C/GPa, which equals 0.0138 ppm C per bar of CH_4 partial pressure. This number is

actually rather similar to that for CO (see above). If one assumes that the solubility data of Ardia *et al.* (2013) may also be applied to a peridotitic melt and neglects a possible temperature dependence, the solubility of methane in a magma ocean may be calculated, as shown in Figure S-1b. The contribution of methane to bulk carbon solubility is very low, below 1 ppm for hydrogen fugacities up to several 100 bar. Such high hydrogen fugacities are, however, implausible for magma ocean temperatures. At a temperature of 2000 K, the average velocity v of a H_2 molecule would be 4.1 km/s, according to the relationship $1/2\ mv^2 = kT$, where k is the Boltzmann constant and m is the mass of H_2. This value is close to the planetary escape velocity for smaller planets such as Mercury (4.2 km/s), but below that for Earth (11.2 km/s). Since there is a statistical distribution of molecular velocities, a significant fraction of H_2 molecules will reach velocities even above the terrestrial escape velocity, such that even for an Earth-size planet, rapid loss of hydrogen to space will occur (e.g. Volkov *et al.* 2011). We therefore conclude that the contribution of methane to bulk carbon solubility in a magma ocean can be ignored under all plausible circumstances.

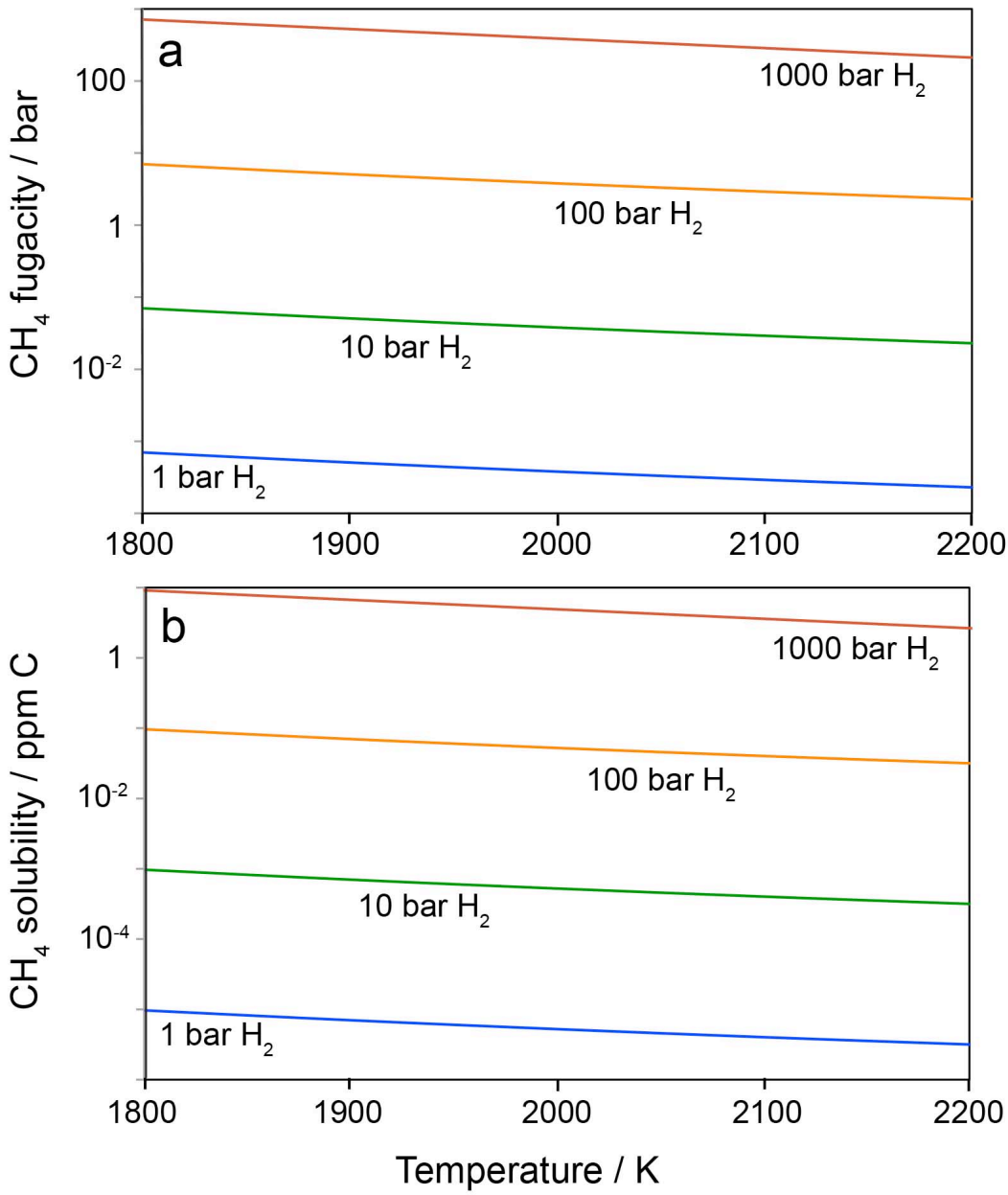

Figure S-1 Methane (CH_4) fugacity (a) and methane solubility in a magma ocean (b) for H_2 fugacities from 1 to 1000 bar and temperatures from 1800 to 2200 K

Possible graphite floatation and formation of a graphite-rich crust on Mercury

Due to its highly reducing nature, planet Mercury may provide a good example for the process of graphite floatation. Namur *et al.* (2016) compared the sulfur concentration in lavas on the surface of Mercury with experimentally determined sulfur solubilities in silicate melts and concluded that they record a log fO_2 of IW-5.4. Somewhat less reducing conditions may be inferred from the low FeO content of the corresponding magmas, with log fO_2 ranging from IW-2.8 to IW-4.5 (Cartier and Wood 2019). At these low oxygen fugacities, our models predict that a large fraction of the total carbon in the planet should precipitate as graphite, rather than being sequestered into the core (Fig. 4 of main text) and floatation of this graphite on the surface of the magma ocean is plausible (Fig. 2 of main text), in particular, if one allows for some sintering of graphite into larger aggregates. This is entirely consistent with the direct detection of a graphite-rich crust on the surface of Mercury by remote-sensing techniques (Peplowski *et al.* 2016).

The possibility of graphite floating on the surface of a Mercurian magma ocean was already raised by van der Kaden and McCubbin (2015) based on simple density arguments. However, they did not investigate the dynamic stability of graphite in a convecting magma ocean, nor did they provide a thermodynamic reason for abundant graphite precipitation. Cartier and Wood (2019) suggested that the carbon enrichment on the surface of Mercury may be due to carbon becoming more lithophile at very reducing conditions. It should be noted that the mechanism in the model presented here is very different. As shown in Figure 3 (main text) and following the model of Chi *et al*. (2014) $D_C^{metal/silicate}$ actually increases continuously under more reducing conditions. The inefficient segregation of carbon into the core is in our model caused by the very low carbon solubility in the silicate melt in equilibrium with floating graphite. The near constancy of the carbon content in metal coexisting with graphite (Fig. 3b, main text) provides an independent thermodynamic test that verifies the assumptions in our model.

The importance of graphite relative to diamond in sequestering carbon from a magma ocean.

Hirschmann (2012) proposed that diamond may precipitate from a magma ocean at greater depth; the diamond may then sink until it remains neutrally buoyant in the magma ocean. In this way, a carbon-enriched layer could be produced in the mantle. While such a process may be conceivable, we consider it to be unlikely for two reasons. (1) The difference in Gibbs free energy between graphite and diamond is small at upper mantle conditions. At given oxygen fugacity, the solubility of solid carbon (graphite or diamond) will therefore be primarily controlled by temperature und pressure. At graphite or diamond saturation, carbon solubility in the melt probably gently decreases with pressure (e.g. Eguchi and Dasgupta 2018), but increases with temperature (see Fig. 3 of the main text). Since the temperature at the surface of the magma ocean is expected to be much lower than deep in its interior, the surface is the most plausible place for carbon precipitation in the form of graphite. Moreover, most of the carbon will be delivered from the beginning as graphite-like material, which is likely dynamically stable on the magma ocean surface (Fig. 2 of the main text). (2) Due to the vanishing density difference between diamond and peridotite melt at the depth of neutral buoyancy, it would likely be re-entrained into the convective currents of the magma ocean, thus no carbon-enriched layer could form.

Supplementary Information References

Ardia, P., Hirschmann, M.M., Withers, A.C., Stanley, B.D. (2013) Solubility of CH_4 in a synthetic basaltic melt, with applications to atmosphere–magma ocean–core partitioning of volatiles and to the evolution of the Martian atmosphere. *Geochimica et Cosmochimica Acta* 114, 52–71

Cartier, C., Wood, B.J. (2019) The role of reducing conditions in building Mercury. *Elements* 15, 39-45.

Eguchi, J., Dasgupta, R. (2018) A CO_2 solubility model for silicate melts from fluid saturation to graphite or diamond saturation. *Chemical Geology* 487, 23–38.

Hirschmann, M.M. (2012) Magma ocean influence on early atmosphere mass and composition. *Earth and Planetary Science Letters* 341-344, 48–57.

Kraichnan, R.H. (1962) Turbulent thermal convection at arbitrary Prandtl number. *Physics of Fluids* 5, 1374–1389.

Liebske, C., Schmickler, B., Terasaki, H., Poe, B.T., Suzuki, A., Funakoshi, K.-I., Ando, R., Rubie, D.C. (2005). Viscosity of peridotite liquid up to 13 GPa: Implications for magma ocean viscosities. *Earth and Planetary Science Letters* 240, 589–604.

Namur, O., Charlier, B., Holtz, F., Cartier, C., Mccammon, C (2016) Sulfur solubility in reduced mafic silicate melts: Implications for the speciation and distribution of sulfur on Mercury. *Earth and Planetary Science Letters* 448, 102-114.

Ni H., Keppler H. (2013) Carbon in silicate melts. *Reviews in Mineralogy and Geochemistry* 75, 251-287.

Priestly, C.H.B. (1959) *Turbulent Transfer in the Lower Atmosphere*. University of Chicago Press, Chicago, IL.

Robie, R.A., Hemingway, B.S. (1995) Thermodynamic Properties of Minerals and Related Substances at 298.15 K and 1 Bar (10^5 Pascals) Pressure and at Higher Temperatures. *US Geological Survey Bulletin* 2131.

Rubie, D.C., Melosh, H.J., Reid, J.E., Liebske, C., Righter, K. (2003) Mechanisms of metal-silicate equilibration in the terrestrial magma ocean. *Earth and Planetary Science Letters* 205, 239-255.

Solomatov, V.S. (2015). Magma oceans and primordial mantle differentiation. In: *Treatise on Geophysics* Vol. 9, 81–104.

Van Der Kaaden, K. E., Mccubbin, F. M. (2015) Exotic crust formation on Mercury: consequences of a shallow, FeO-poor mantle. *Journal of Geophysical Research* 120, 195-209.

Volkov, A., Johnson, R.E.Tucker, O.J., Erwin, J.T. (2011) Thermally driven atmospheric escape: transition from hydrodynamic to jeans escape. *The Astrophysical Journal Letters* 729, L24.

Yoshioka, T., Nakashima, D., Nakamura, T., Shcheka, S., Keppler, H. (2019) Carbon solubility in silicate melts in equilibrium with a CO-CO_2 gas phase and graphite. *Geochimica et Cosmochimica Acta* 259, 129-143.